

Characterising hot stellar systems with confidence

Souradeep Chattopadhyay,¹ and Ranjan Maitra,¹[★]

¹ *Department of Statistics, Iowa State University, 2438, Osborn Drive, Ames, Iowa 50011-1090, USA*

Accepted XXX. Received YYY; in original form ZZZ

ABSTRACT

Hot stellar systems (HSS) are a collection of stars bound together by gravitational attraction. These systems hold clues to many mysteries of outer space so understanding their origin, evolution and physical properties is important but remains a huge challenge. We used multivariate-*t*-mixtures model-based clustering to analyze 13456 hot stellar systems from Misgeld & Hilker (2011) that included 12763 candidate globular clusters and found eight homogeneous groups using the Bayesian Information Criterion (BIC). A nonparametric bootstrap procedure was used to estimate the confidence of each of our clustering assignments. The eight obtained groups can be characterized in terms of the correlation, mass, effective radius and surface density. Using conventional correlation-mass-effective radius-surface density notation, the largest group, Group 1, can be described as having positive-low-low-moderate characteristics. The other groups, numbered in decreasing sizes are similarly characterised, with Group 2 having positive-low-low-high characteristics, Group 3 displaying positive-low-low-moderate characteristics, Group 4 having positive-low-low-high characteristic, Group 5 displaying positive-low-moderate-moderate characteristic and Group 6 showing positive-moderate-low-high characteristic. The smallest group (Group 8) shows negative-low-moderate-moderate characteristic. Group 7 has no candidate clusters and so cannot be similarly labeled but the mass, effective radius correlation for these non-candidates indicates that they are larger than typical globular clusters. Assertions drawn for each group are ambiguous for a few HSS having low confidence in classification. Our analysis identifies distinct kinds of HSS with varying confidence and provides novel insight into their physical and evolutionary properties.

Key words: methods: statistical – Astronomical instrumentation, methods, and techniques; methods: data analysis – Astronomical instrumentation, methods, and techniques; Galaxy: globular clusters: general – The Galaxy

1 INTRODUCTION

Over the past years scientists have identified several stars, galaxies and other stellar objects that they believe hold clues to understanding the origin and other mysteries of outer space. Hot stellar systems (HSS) form one such class celestial objects and consist of globular clusters, nuclear star clusters, compact elliptical galaxies, giant elliptical galaxies, ultra compact dwarf elliptical galaxies, nuclear star clusters and so on. These HSS are very important to understand important events of outer space like star or blackhole formation, evolution of galaxies and so on. Indeed, the physical properties of these objects have been directly linked to galaxy interactions and have been extensively studied over the past many years. Consequently there are many theories to explain these dynamic stellar objects (Chattopadhyay & Karmakar 2013). One of the most popular notions (Burstein et al. 1997;

Bernardi et al. 2003; Kormendy et al. 2009; Misgeld & Hilker 2011) in studying these objects are the fundamental plane relations (Brosche 1973). These planes are typically constructed with parameters such as luminosity, surface brightness, stellar magnitude or central velocity dispersion and have helped in understanding important properties of these stellar objects. Jordán et al. (2008) catalogued and studied 12763 candidate globular clusters (GCs) from the Virgo Cluster Survey during the eleventh Hubble Space Telescope observation cycle while Misgeld & Hilker (2011) catalogued an additional 693 additional HSS. These HSS were analyzed by Chattopadhyay & Karmakar (2013) to study the origins of ultra compact and ultra faint dwarf galaxies. The authors pointed out that several studies had previously compared stellar objects such as GCs and dwarf spheroidals, these investigations had only used two-point correlations between different projections of the fundamental plane of galaxies. A multivariate analysis of data might uncover more information about these HSS, so Chattopadhyay & Karmakar (2013)

★ E-mail: maitra@iastate.edu (RM)

used k -means clustering with the jump statistic (Sugar & James 2003) and found five and four homogeneous groups in the 693 non-candidate and the larger 13456 HSS datasets.

Clustering (Kettenring 2006; Xu & Wunsch 2009; Everitt 2011) is an unsupervised learning technique that groups observations without a response variable. While there are many kinds of clustering algorithms, they are broadly categorized into hierarchical and non-hierarchical approaches. Hierarchical clustering algorithms result in a tree-like grouping hierarchy while non-hierarchical algorithms such as k -means or model-based clustering (MBC) typically optimize an objective function using iterative greedy algorithms – these algorithms typically require a specified number of groups. The objective function is often multimodal and requires careful initialization (Maitra 2009). For a detailed review on model-based clustering see Melnykov & Maitra (2010). Parameter estimation in clustering accompanied by uncertainty in those estimates and careful assessment of these estimates is often required to judge the efficacy of the obtained estimates. Thus it is important to assess the uncertainty in the obtained groupings. An effective way of analyzing this uncertainty is by calculating the confidence of classification probabilities of each data point. We use a nonparametric bootstrap procedure here to calculate this uncertainty.

The rest of this paper is organised as follows. Section 2 provides an overview of the dataset used for analysis and details how the parameters used in our analysis are derived. It further discusses the statistical properties of the parameters in the HSS used in our analysis. Section 3 briefly outlines MBC using a mixture of multivariate- t densities and the EM method of estimating the parameters of the mixture model. Section 4 discusses the groups and the confidence with which we classify each HSS in their respective groups. We also investigate the physical and evolutionary properties of these groups here. The paper concludes with some discussion.

2 DESCRIPTION OF DATA

The dataset used in our analysis is from Misgeld & Hilker (2011) and contains 13456 hot stellar systems of different types like globular clusters (GC), giant ellipticals (gE), compact ellipticals (cE), ultra compact dwarf galaxies (UCD), dwarf globular transition objects (DGTO), nuclear of star clusters (NuSc), bulges of spiral galaxy (Sbul), nuclei of nucleated dwarf galaxies (dE,N) compiled from different sources. The dataset also includes 12763 candidate GCs (GC_VCC) from the Virgo Globular Cluster survey: it is unclear whether these candidate HSS are GCs. Chattopadhyay & Karmakar (2013) excluded these candidate GCs from their initial and primary analysis, focusing largely on the 673 non-candidate HSS. We propose to comprehensively analyse all 13456 HSS that includes the 12763 HSS. The parameters in Misgeld & Hilker (2011) are stellar mass (M_s), effective radius (R_e), mass surface density averaged over projected effective radius (S_e) and absolute magnitude in the V band (M_v). Following Chattopadhyay & Karmakar (2013) we use the logarithm of M_s , R_e and the mass to luminosity ratio (M_s/L_v) in solar luminosity ($M_{s,\odot}$) units in the logarithmic scale (base 10) for our analysis. The M_s/L_v ratio was ob-

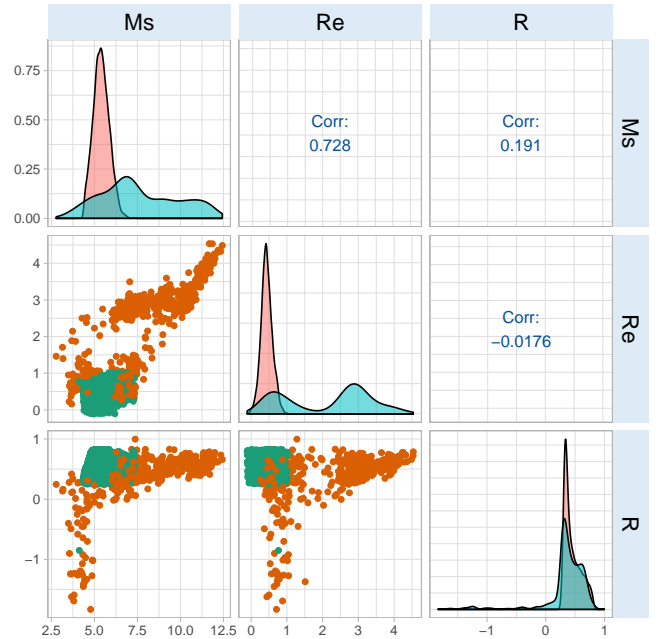


Figure 1: Pairwise scatterplots, estimated densities and correlation coefficient of the logarithm of the parameters in our dataset. Here M_s denotes mass, R_e effective radius and R the mass-luminosity ratio. In the scatterplot, orange indicates the non candidates and green the candidates. For the density plots the blue curves represent the non candidates. Note that the calculated correlations are for all 13456 HSS in the dataset (including the non-candidates and candidates).

tained using the standard magnitude-luminosity relation

$$\frac{M_s}{M_{s,\odot}} = -2.5 \left(\frac{L_v}{L_{v,\odot}} \right) \quad (1)$$

where $L_{v,\odot}$ denotes the luminosity of the sun. The $\log_{10} S_e$ is taken into account while interpreting the results but are not used in the clustering mechanism. Figure 1 provides the pairwise scatterplots of the three parameters for both candidate and non-candidate objects along with the density plot of the parameters for both candidates and non candidates used in clustering. From Figure 1 we see that the densities of the non-candidates display moderate bimodality especially effective radius and mass-luminosity ratio. There is therefore evidence of grouping, certainly in each parameter. Also, the correlations signify that mass and effective radius are moderately positively correlated, as typically expected in stellar objects. But mass-luminosity ratio has a weak linear association with both mass and effective radius. In the next sections, we therefore investigate robust model-based clustering methods for finding the kinds of HSS in the dataset and study their properties.

3 METHODOLOGY

3.1 MBC using a mixture of multivariate- t densities

MBC provides a principled way to find homogeneous groups in a given dataset. As mentioned in Section 2 it scores over

classical clustering algorithms like k -means due to its ability to better model the heterogeneity in the that may be present in the groups. As pointed out by [Chattopadhyay & Maitra \(2017\)](#) the assumption of spherically dispersed homogeneous groups when such assumption is not valid can lead to erroneous results. In MBC ([Melnykov & Maitra 2010](#); [McLachlan & Peel 2000](#)) the observations X_1, X_2, \dots, X_n are assumed to be realizations from a G -component mixture model ([McLachlan & Peel 2000](#)) with probability density function (PDF)

$$f(x; \theta) = \sum_{g=1}^G \pi_g f_g(x; \eta_g) \quad (2)$$

where $f_g(\cdot; \eta_g)$ is the density of the g th group, η_g the vector of unknown parameters and $\pi_g = \Pr[x_i \in \mathcal{G}_g]$ is the mixing proportion of the g th group, $g = 1, 2, \dots, G$, and $\sum_{g=1}^G \pi_g = 1$. The component density $f_g(\cdot; \eta_g)$ can be chosen according to specific application with the most popular choice being the multivariate Gaussian density ([Chattopadhyay & Maitra 2017](#); [Fraley & Raftery 1998, 2002](#)). Another useful family of mixture models proposed by [McLachlan & Peel \(1998\)](#) specifies $f_g(\cdot; \eta_g)$ to be the multivariate- t density. That is,

$$f_g(z; \mu_g, \Sigma_g, \nu_g) = \frac{\Gamma(\nu_g + p)/2}{\Gamma(\nu_g/2) \nu_g^{\frac{p}{2}} \pi_g^{\frac{p}{2}} |\Sigma_g|^{\frac{1}{2}}} \left[1 + \frac{1}{\nu_g} (z - \mu_g)^T \Sigma_g^{-1} (z - \mu_g) \right], \quad (3)$$

for $z \in \mathbb{R}^p$, where μ_g denotes the mean vector, Σ_g the scale matrix and ν_g the degrees of freedom, all for the g th mixture component, $g = 1, 2, \dots, G$. Our analysis uses the multivariate- t mixture (t MM) model (instead of the Gaussian mixture model) because the multivariate- t MM better accounts for the tails in the component densities of the mixture under consideration. Subsequent steps in clustering involve obtaining maximum likelihood estimates of the parameters η_g , $g = 1, 2, \dots, G$ using the Expectation Maximization algorithm ([Dempster et al. 1977](#); [McLachlan & Krishnan 2008](#); [Chattopadhyay & Maitra 2017](#); [Chattopadhyay & Maitra 2018](#)) and assigning each individual observation based on the maximum posterior probability that it belongs to a given group. We use BIC ([Schwarz 1978](#); [Chattopadhyay & Maitra 2017](#)) to decide on G . From now, on we use t MMBC to refer to t MM-based clustering.)

4 CLUSTER ANALYSIS OF HSS

4.1 t MMBC using three parameters

We performed G -component t MMBC, for $G \in \{1, 2, \dots, 9\}$, using the `teigen` package in R on M_s , R_e and the M_s/L_v , all in the \log_{10} -scale, of the 13456 HSS. Figure 2 indicates that a eight-component t MM provides an optimal fit as per BIC. Our results are different from that of [Chattopadhyay & Karmakar \(2013\)](#) who using k -means found five groups when excluding the candidate globular clusters of [Jordán et al. \(2008\)](#) and four groups when including them all. Also the best model from the large class of `teigen` family obtained by constraining the dispersion matrices is also selected using BIC.

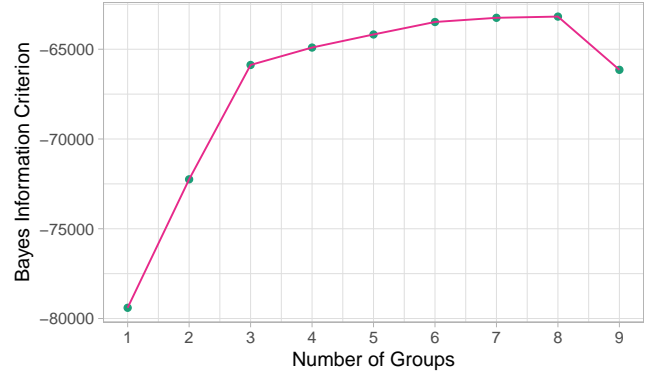


Figure 2: BIC for each G upon performing G -component t MMBC with 13456 HSS from [Misgeld & Hilker \(2011\)](#).

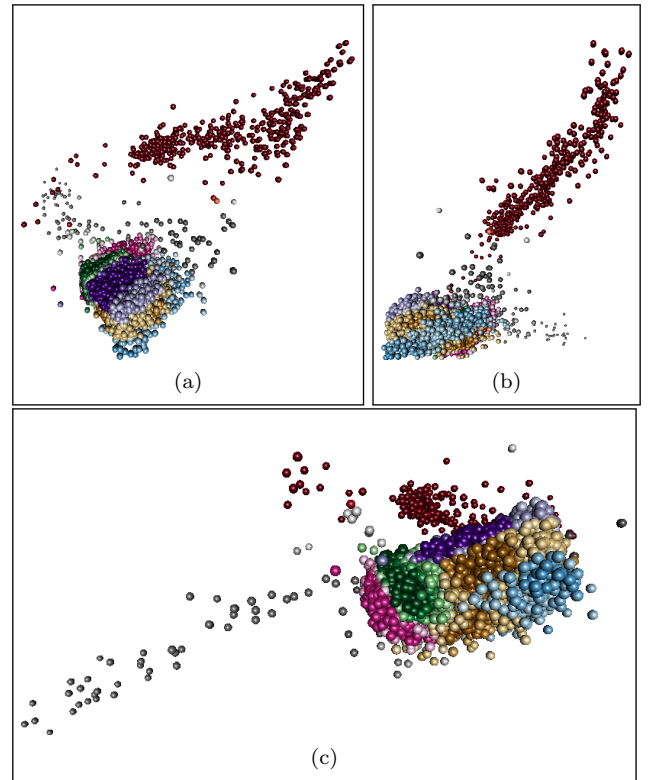


Figure 3: Three viewing angles of the scatterplot of the full dataset with different colors representing different groups and intensity of the color signifying the underlying confidence in that particular grouping. Darker shades indicate higher confidence of classification of that particular object.

Figure 3 provides a 3D scatterplot of the eight t MMBC groups obtained on the 13456 HSS. (For greater clarity, 3D scatterplots of Groups 2 and 6, Groups 3 and 5, Groups 1 and 4, Groups 1, 3 and 8 are presented, a little later, in Figures 6, 8, 7, 9 to highlight the differences in these pairs of groups.)

4.2 Validity of the obtained groupings

This section carefully analyzes the quality of our obtained groupings using an approximate pairwise overlap measure (Maitra & Melnykov 2010; Melnykov & Maitra 2011; Melnykov et al. 2012) between two groups. The pairwise overlap provides us with a sense of the distinctiveness between groups obtained using a particular clustering method. These values lie inside $[0, 1]$ with values closer to 1 indicating that the two groups are poorly separated.

Apart from the overlap measure we also obtained the uncertainty in our groupings by calculating the confidence of classification of each HSS using a nonparametric bootstrap. The bootstrap confidence of classification (BCC) helps us analyze the chance that a particular HSS has been wrongly classified to a group that is different from its original. BCC values are between 0 and 1, with values closer to 1 indicating greater chance that a given HSS has been classified correctly. Our exact nonparametric bootstrapping procedure is detailed in Section 4.2.2.

4.2.1 Measuring distinctiveness using the pairwise overlap

The empirical pairwise overlap measures (Maitra & Melnykov 2010) to characterise the distinctiveness of the eight groups obtained by the eight-component t MMBC can be obtained using the R package *MixSim* (Melnykov et al. 2012) or the C package *CARP* (Melnykov & Maitra 2011). These values are displayed in Figure 4. The overlap map indicates that

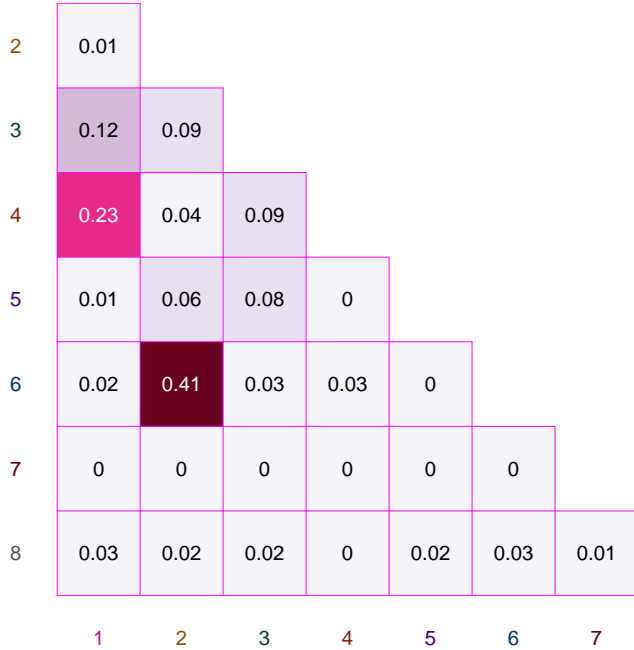


Figure 4: Pairwise overlap measures between any two groups obtained by our eight-component t MMBC solutions.

Group 7 has negligible overlap with all groups other than Group 8 with which it has marginal overlap. Also Group 6 has negligible overlap with Groups 5 and 7 as does Group 5 with Groups 4, 7 and 8. Group 4 also has negligible overlap with Group 8. The highest overlap is between Groups

2 and 6 while Groups 1 and 4 also have high overlap and low distinctiveness. There is little overlap between the other groups. Overall most groups have very little to negligible overlap and this provides us with well-demarcated groups in most cases.

4.2.2 Measuring uncertainty in the obtained groupings through bootstrapping

We assess the uncertainty in the parameter estimates and the corresponding classification using a nonparametric bootstrap technique where we repeatedly resample from the dataset with replacement and each resample is analyzed to obtain estimates of the parameters of interest. For a detailed study on the bootstrap refer to Efron (1979).

In our scenario, the parameters of interest are the group memberships and a good cluster analysis is expected to produce the same group memberships for most of the data points at each bootstrap replicate. The following procedure describes our steps for obtaining the confidence of classification for each observation.

(i) First we perform t MMBC of the original 13456 HSS as described in Section 2. This matches the analysis done so far and yields 8 t MMBC groups.

(ii) Sample 13456 HSS from the data with replacement and repeat t MMBC on the sampled data using the classifications obtained in step (i) as the initial estimates for the groupings. Repeat this procedure B times to obtain B sets of classification estimates. Let us denote these B sets by C_1, C_2, \dots, C_B . Also let C_{ij} denote the classification of the j th data point in the i th bootstrap replicate, where $i = 1, 2, \dots, B$ and $j = 1, 2, \dots, 13456$.

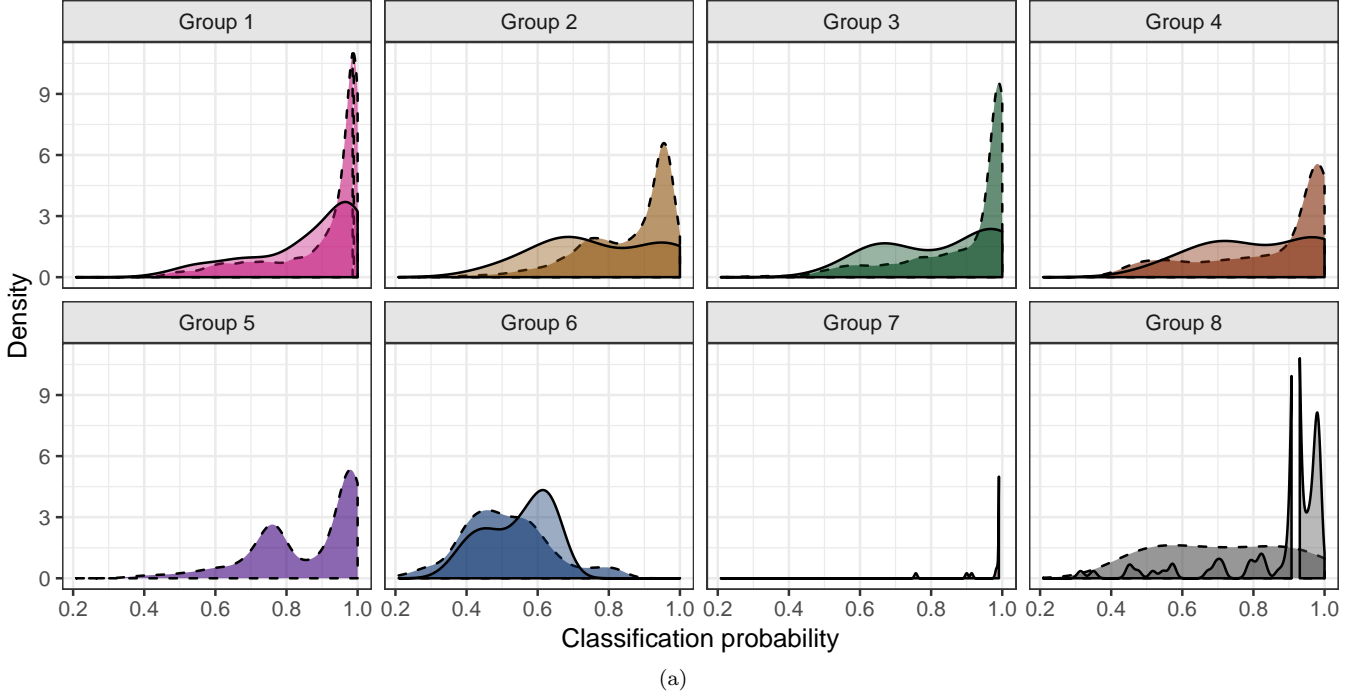
(iii) The classification probability for the j th data point is obtained as

$$p_j = \frac{1}{B} \sum_{i=1}^B C_{ij} \quad (4)$$

where $j = 1, 2, \dots, 13456$. In our analysis, we took $B = 1000$, that is, we resampled 1000 times from the dataset.

Figure 5 provides a density plot of the classification probabilities for each of the eight groups for both the candidate and non-candidate HSS and a tabulation of the number of candidate and non candidate HSS in each of the eight groups with confidences in each the seven intervals $(0, 0.30]$, $(0.30, 0.60]$, $(0.60, 0.85]$, $(0.85, 0.9]$, $(0.9, 0.95]$, $(0.95, 1]$. It is clear that with the exception of Group 1, all other groups have HSS with high or very high BCC. This indicates that our clustering method has worked well in allocating the candidate globular clusters to their respective groups.

We end our discussion in this section by noting that we could have also obtained an estimate of the confidence of classification based on the posterior probability of classification. However, we use a nonparametric bootstrap technique for estimating the classification probabilities in order to account for the uncertainty in the modeling and to guard against possible model misspecification. The choice of the nonparametric bootstrap technique provides us with more robust estimates of the confidence of classification compared to using posterior probability because it accounts for modeling errors to be included in the calculation of the classification confidence.



| Group | (0, 0.30] | | (0.30, 0.60] | | (0.60, 0.80] | | (0.80, 0.85] | | (0.85, 0.90] | | (0.90, 0.95] | | (0.95, 1] | |
|-------|-----------|----|--------------|----|--------------|----|--------------|----|--------------|----|--------------|----|-----------|-----|
| | C | NC | C | NC | C | NC | C | NC | C | NC | C | NC | C | NC |
| 1 | | | 183 | 8 | 516 | 16 | 166 | 7 | 241 | 11 | 458 | 10 | 2096 | 36 |
| 2 | | | 156 | 1 | 882 | 5 | 268 | | 342 | | 654 | 1 | 1107 | 3 |
| 3 | 4 | | 198 | 1 | 410 | 6 | 144 | 1 | 187 | 1 | 236 | 1 | 1635 | 7 |
| 4 | | | 224 | 1 | 242 | 3 | 85 | 1 | 86 | | 129 | | 750 | 4 |
| 5 | | | 53 | | 280 | | 32 | 1 | 40 | | 64 | | 403 | |
| 6 | 19 | | 369 | 21 | 80 | 12 | 14 | | | | | | | |
| 7 | | | | | | 1 | | | | 1 | | 1 | | 415 |
| 8 | | | 3 | 9 | 3 | 7 | 1 | 5 | | 3 | 2 | 63 | 1 | 30 |

(b)

Figure 5: (a) Distribution of the BCCs of both candidate and non-candidate HSS for each of the eight groups. Dotted lines and lighter shades indicate candidates while solid lines and darker shades indicate non-candidate HSS. (b) Number of candidate HSS (C) and non-candidate HSS (NC) having confidences in each of the seven intervals for each of the t MMBC eight groups. Here $(\alpha, \beta]$ denotes the interval with left endpoint α (not included) and right endpoint β (included). The number of candidate HSS in Group 5 is not enough to obtain a density plot and is omitted.

We now proceed to analyze the groups obtained using t MMBC and also study their physical and evolutionary properties.

4.3 Analysis of results

4.3.1 Properties of Identified Groups

Tables 1 and Figure 5 display the number of HSS in each of the eight groups obtained by t MMBC and also the number of HSS in each group at different levels of BCC. The mean values of the parameters for each group are in Table 2. Apart from this the correlation between the mass and effective radius of the candidate objects for each of the eight t MMBC groups are displayed in Table 3. A density plot of

| Group | 1 | 2 | 3 | 4 | 5 | 6 | 7 | 8 |
|-------|------|------|------|------|-----|-----|-----|-----|
| # HSS | 3748 | 3419 | 2831 | 1525 | 873 | 515 | 418 | 127 |

Table 1: Frequency of HSS in each of the eight t MMBC groups.

the classification probabilities of both candidate and non-candidate HSS for each of the eight groups is also presented in Figure 5(a). From this figure, it is evident that for all the eight groups the classification probabilities both for candidates and non-candidates exhibit some bimodality. This is especially true of Groups 5 and 8. Further, the highest peaks for all these groups except Group 6 lie closer to 1 indicating

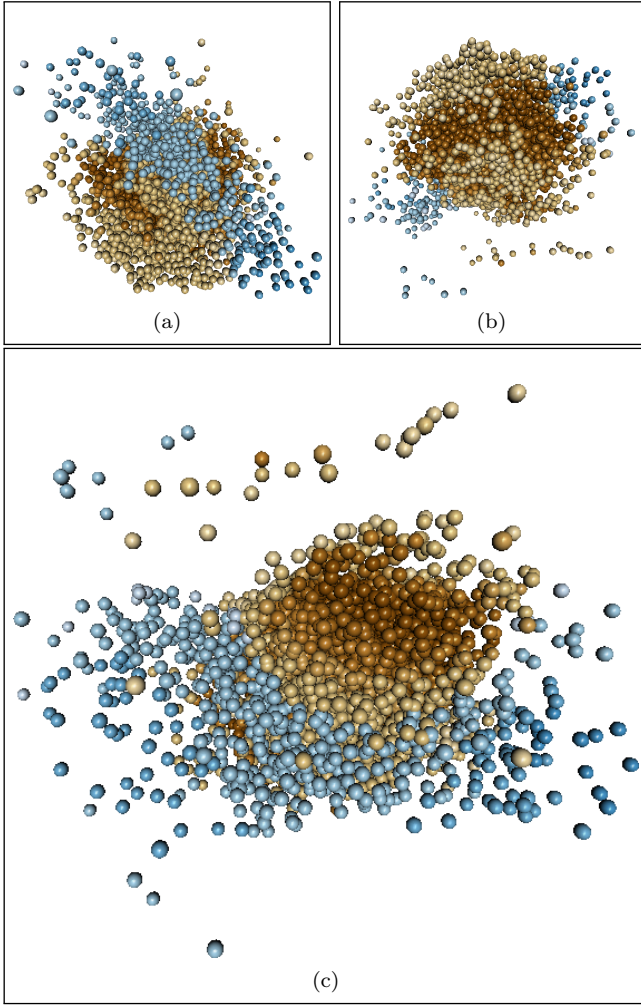


Figure 6: 3D scatterplots of Groups 2 and 6 having pairwise overlap 0.41 and color and shading mechanism same as Figure 3.

| Group | M_V | R_e | M_s | S_e | M_V/L_V |
|-------|--------|-------|-------|-------|-----------|
| 1 | -7.651 | 0.475 | 5.313 | 3.565 | 2.094 |
| 2 | -7.577 | 0.348 | 5.556 | 4.062 | 4.023 |
| 3 | -6.905 | 0.470 | 5.01 | 3.362 | 2.559 |
| 4 | -8.609 | 0.408 | 5.744 | 4.131 | 2.341 |
| 5 | -6.432 | 0.641 | 5.134 | 3.053 | 4.408 |
| 6 | -9.107 | 0.331 | 6.184 | 4.723 | 4.215 |
| 7 | -16.05 | 3.032 | 8.817 | 1.954 | 3.105 |
| 8 | -9.711 | 0.991 | 5.803 | 3.023 | 2.131 |

Table 2: Mean parameter values for each of the eight *t*MMBC groups.

that most HSS have high BCC into their groups. Further, Table 2 shows that Group 5 has the highest average absolute magnitude, while Group 7 has the lowest mean absolute magnitude. The effective radius is on the average the highest for HSS in Group 7 and lowest for Group 6. Group 7 also consists of HSS having the highest average stellar mass, while Group 3 has the lowest average stellar mass. The mean mass

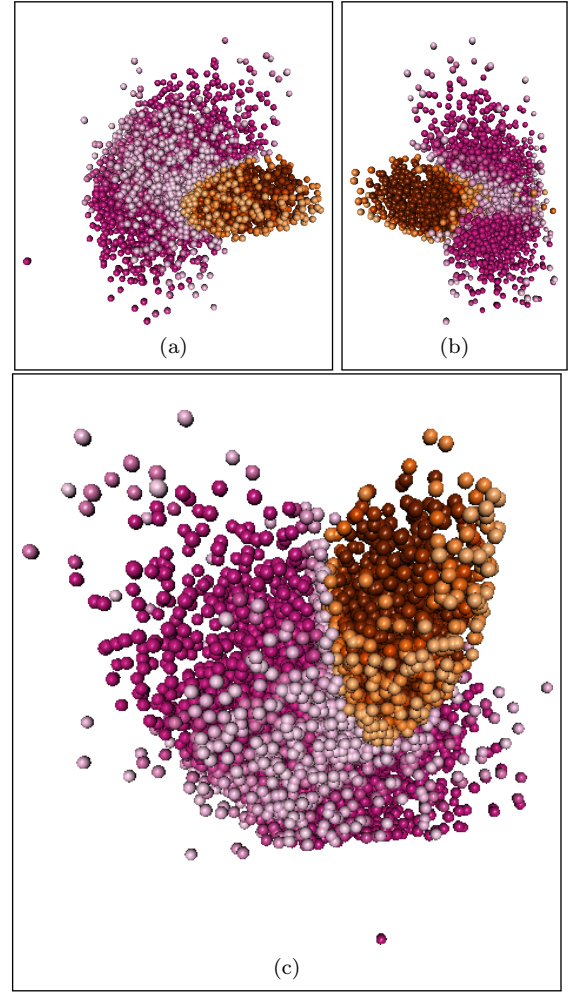


Figure 7: 3D scatterplots of Groups 1 and 4 having pairwise overlap 0.23 and color and shading mechanism same as Figure 3.

| Group | 1 | 2 | 3 | 4 | 5 | 6 | 8 |
|-------------|-------|-------|-------|-------|-------|-------|--------|
| Correlation | 0.348 | 0.016 | 0.275 | 0.149 | 0.723 | 0.579 | -0.460 |

Table 3: Correlation between mass and effective radius of the candidate GCs in each *t*MMBC group. (Group 7 has no candidate GCs.)

surface density is highest in Group 6 and lowest in Group 7. The average mass-luminosity ratio is highest in Group 5 and lowest in Group 1. These properties can be used to get an intuitive idea about the physical and evolutionary properties of these HSS and will be discussed in more detail next.

4.3.2 Interpretations

Here we try to understand the physical and evolutionary properties of the objects in each of the eight groups using the stellar mass and surface density. Typically we try to ascertain the physical and evolutionary properties of the GC_VCCs in each group by looking at the correlation between mass and effective radius apart from their mass and

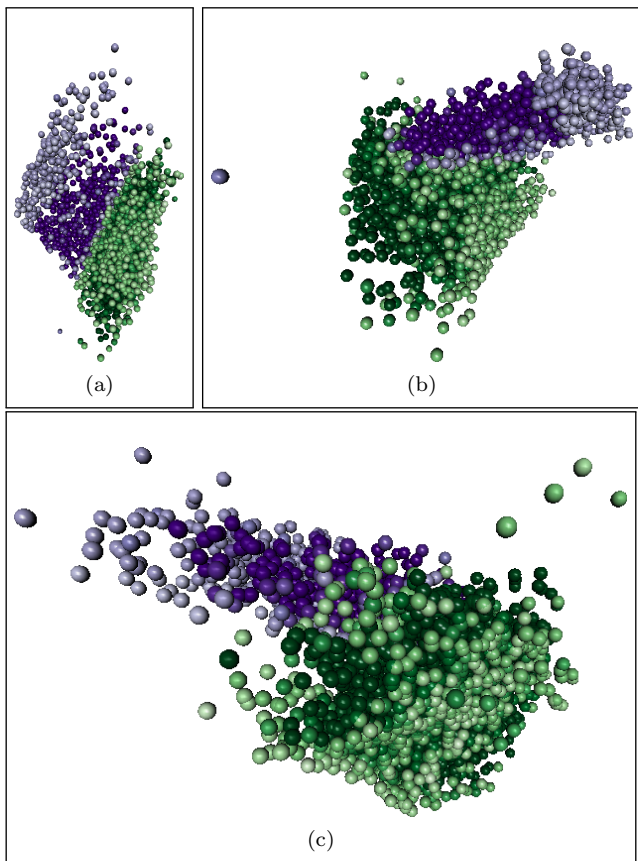


Figure 8: 3D scatterplots of Groups 3 and 5 having pair-wise overlap 0.08 and color and shading mechanism same as Figure 3.

surface density. Based on these properties we can typically characterise each group using the conventional correlation-mass-effective radius-surface density, where positive correlation indicates that the GC_VCCs in that group are larger than the typical globular clusters and a negative correlation indicates that the GC_VCCs in that group are typical globular clusters and lie on the outer halo of their respective galaxies (Gieles et al. 2010). Stellar mass is typically low, moderate or high depending on the group. Like stellar mass, effective radius and surface density are also either low, moderate or high. Also, importantly, except for the 7th group, all the groups contain a sizeable number of GC_VCC. We now discuss the characteristics of each group (which are numbered in decreasing size) specifically.

Group 1 contains the highest number of GC_VCCs is also dominated by GCs. The correlation between mass and effective radius for the GC_VCCs in this group is positive. This means that the GC_VCCs in this group may be larger than typical GCs, that is, they might be UCDs. The HSS in this group have a low effective radius and a moderate surface density. This implies that the mass per unit area of the HSS in this group are quite moderate. Thus we can hypothesize that the stellar objects in the GC_VCC's for this group lie near or on the main sequence of the HR diagram. The same can be asserted for the non- candidate HSS in this group. The stellar mass is also moderate for these objects because of which we can hypothesize that the HSS in this group might

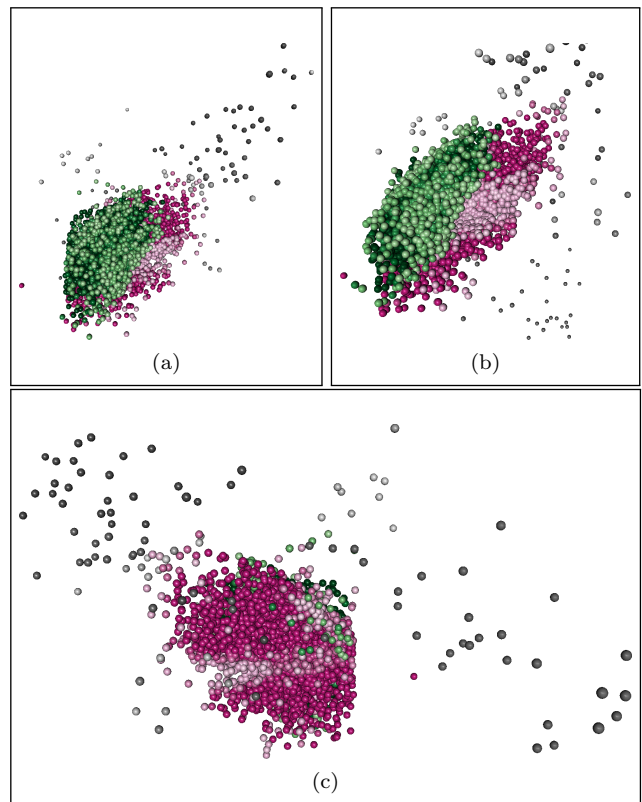


Figure 9: 3D scatterplots of Groups 1, 3 and 8 having color and shading mechanism same as Figure 3.

cool off gradually to become a white dwarf and then become a black dwarf over time and so move to a downward position in the HR diagram. This assertion is less uncertain for the 183 GC_VCCs that are in the range $(0.30, 0.60]$ since these objects have a lower confidence of classification. We can thus label Group 1 as positive-low-low-moderate. Also, since Group 1 has some overlap with Group 4, the assertions for the objects with small confidence of classification in Group 1 may be a little ambiguous but still one can assert that they are larger in size than typical globular clusters (if not UCDs).

Group 2 has low effective radius, low mass and a high surface density. Thus we can hypothesize that the evolutionary path for the objects in this group will be typically similar to that of Group 1 HSS although one can think that the pace of evolution for the objects will be different than that of Group 1 since they have larger surface density. Also correlation between mass and effective radius is positive which signifies that these objects are larger than typical GCs. Thus we can label this group as positive-low-low-high.

The properties of Group 3 are also close to those of Group 1 due to which we can hypothesize similar assertions about Group 3 as that of Group 1. This group can thus be labeled as positive-low-low-moderate. Also there is a small amount of overlap between these two groups which sheds some light as to why these two groups have similarities between them. The pace of evolution can be a little different in Group 3 compared to that in Group 1 because of the small difference in the stellar masses of the two groups. However, this pace may not be substantially different for the

two groups because their stellar mass and effective radius are quite close.

Assertions similar to Group 2 can be also hypothesized for HSS in Group 4. This group is labeled as positive-low-low-high. The pace of evolution can be anticipated to be a little different because of a small significant difference between the stellar mass and effective radius of the two groups.

The HSS assigned to Group 5 have moderate effective radii, low mass and moderate surface density. We can hypothesize that the structure of stellar evolution for Group 5 is similar to that of Group 1 although we can expect that the pace of evolution is different for these two groups since Group 5 has a comparatively higher effective radius than Group 1. Further the HSS in this group are larger than typical globular clusters because of positive correlation between mass and effective radius. We label this group as positive-low-moderate-moderate.

The stellar objects in Group 6 have a positive correlation signifying that the HSS in this group are larger than typical GCs. Apart from this the objects in this group have the highest surface density, moderate mass and very low effective radii. This can suggest destabilization of their cores due to which they will collapse under their own gravity to become a neutrino star or a black hole. But any assertions about the candidates in Group 6 are ambiguous since most of the candidates in this group have low confidence of classification. We label this group as positive-moderate-low-high with a caution that this labelling may be ambiguous. Also note that Group 6 has high overlap with Group 2. So characteristics of the objects in Group 2 might also be reflected for the objects of Group 6 in the overlapping region.

The non-candidate stellar objects of Group 7 have high stellar mass (in fact the highest stellar mass amongst all the groups) but low surface density (also lowest among all the groups). Thus it is unlikely for the stars in these systems to collapse under its own gravity to create black holes. They may move upwards in the HR diagram to become a red giant due to their low surface density and then ultimately trigger a supernova. Since this group has no candidate clusters we are unable to label it as per the rules set for the other groups. But the non-candidate objects in this group have a positive correlation and so the objects here can be asserted to be larger in size than typical globular clusters.

The smallest group (Group 8) has negative correlation between mass and effective radius, indicating that the HSS here are typical globular clusters and lie on the outer halo of their respective galaxies. The moderate radius, low mass and moderate surface density indicate that these HSS lie on or near the main sequence and are in a stable state of evolution. This group is labelled as negative-low-moderate-moderate according to our classification scheme.

Our analysis has shed some light on the nature of these systems, including and especially, on the non-candidate HSS. This can help provide more insight into the characteristics of these systems and help identify the appropriateness of classifying them into one of the classes of known systems, although doing so would require more detailed analysis of these objects using additional astronomical and data analysis techniques.

5 CONCLUSIONS

Chattopadhyay & Karmakar (2013) clustered 673 HSS from Misgeld & Hilker (2011) to find homogeneous groups amongst them. Using the popular k -means clustering algorithm and the jump statistic for selection of optimal number of groups they arrived at 5 optimal groups whose properties were explored using fundamental plane relations and other physical parameters. In their main analysis they excluded the candidate GCs, claiming that the candidate clusters would render the data unfit for typical clustering algorithms. Their analysis hinges on the homogeneous spherically-dispersed-groups assumption that underlies the k means algorithm, but may not be appropriate and can lead to erroneous results when this assumption does not hold. Our analysis grouped all 13456 HSS of Misgeld & Hilker (2011) using t MMBC and used BIC to optimally find 8 groups. Using a nonparametric bootstrap technique we further determined the confidence of classification of each of the 13456 HSS to understand the quality of our clustering algorithm and also to ascertain how correctly the candidate clusters been assigned to their correct groups. The bootstrap results along with the overlap map provide confidence in much of our groupings for the HSS. We then studied the physical and evolutionary properties of the objects in each group by analyzing the mean stellar mass, surface density and effective radius of each group along with the correlation between mass and effective radius for the candidate globular clusters (GC_VCCs) further labeling the groups following the convention correlation-mass-effective radius-surface density. Group 1, the largest group got the label positive-low-low-moderate while Group 2 received the label positive-low-low-high. Group 3 got labelled as positive-low-low-moderate, Group 4 as positive-low-low-high while Group 5 received the label positive-low-moderate-moderate. Group 6 got labelled as positive-moderate-low-high. Since Group 7 does not have any candidate clusters we were unable to assign it a label but our analysis indicated that HSS in this group are larger than typical GCs. The smallest group, Group 8 was labelled as negative-low-moderate-moderate.

There are a number of issues that can merit further investigation. For example it would be useful to explore if the logarithmic transformation used on the parameters is plausible or is obfuscating the clusters. There some other transformation that might lead to better separated groups. This analysis might also be extended for datasets from other sources to analyze whether similar results hold for the HSS for the different datasets from different sources. Also with the availability of information like temperature and color indices of the stars present in the system it might be possible to obtain deeper understanding of the evolution of these systems possibly through HR diagrams. Thus we see that while our analysis has provided some interesting insight into the different types of HSS, additional issues remain that deserve further attention.

ACKNOWLEDGEMENTS

We sincerely thank Professor Tanuka Chattopadhyay for providing us with the dataset of Chattopadhyay & Karmakar (2013).

REFERENCES

- Bernardi M., et al., 2003, *AJ*, **125**, 1866
- Brosche P., 1973, *A&A*, **23**, 259
- Burstein D., Bender R., Faber S., Nolthenius R., 1997, *AJ*, **114**, 1365
- Chattopadhyay T., Karmakar P., 2013, *New Astronomy*, **22**, 22
- Chattopadhyay S., Maitra R., 2017, *Monthly Notices of the Royal Astronomical Society*, **469**, 3374
- Chattopadhyay S., Maitra R., 2018, *MNRAS*, **481**, 3196
- Dempster A. P., Laird N. M., Rubin D. B., 1977, *Journal of the Royal Statistical Society, Series B*, **39**, 1
- Efron B., 1979, *Ann. Statist.*, **7**, 1
- Everitt B., 2011, *Cluster analysis*. Wiley, Chichester, West Sussex, U.K, doi:10.1002/9780470977811
- Fraley C., Raftery A. E., 1998, *The Computer Journal*, **41**, 578
- Fraley C., Raftery A. E., 2002, *Journal of the American Statistical Association*, **97**, 611
- Gieles M., Baumgardt H., Heggie D. C., Lamers H. J. G. L. M., 2010, *Monthly Notices of the Royal Astronomical Society: Letters*, **408**, L16
- Jordán A., et al., 2008, *The Astrophysical Journal Supplement Series*, **180**, 54
- Kettenring J. R., 2006, *Journal of Classification*, **23**, 3
- Kormendy J., Fisher D. B., Cornell M. E., Bender R., 2009, *ApJS*, **182**, 216
- Maitra R., 2009, *IEEE/ACM Transactions on Computational Biology and Bioinformatics*, **6**, 144
- Maitra R., Melnykov V., 2010, *Journal of Computational and Graphical Statistics*, **19**, 354
- McLachlan G., Krishnan T., 2008, *The EM Algorithm and Extensions*, second edn. Wiley, New York, doi:10.2307/2534032
- McLachlan G. J., Peel D., 1998, in Amin A., Dori D., Pudil P., Freeman H., eds, *Advances in Pattern Recognition: Joint IAPR International Workshops SSPR'98 and SPR'98 Sydney, Australia, August 11–13, 1998 Proceedings*. Springer Berlin Heidelberg, Berlin, Heidelberg, pp 658–666, doi:10.1007/BFb0033290
- McLachlan G., Peel D., 2000, *Finite Mixture Models*. John Wiley and Sons, Inc., New York, doi:10.1002/0471721182
- Melnykov V., Maitra R., 2010, *Statist. Surv.*, **4**, 80
- Melnykov V., Maitra R., 2011, *Journal of Machine Learning Research*, **12**, 69
- Melnykov V., Chen W.-C., Maitra R., 2012, *Journal of Statistical Software*, **51**, 1
- Misgeld I., Hilker M., 2011, *Monthly Notices of the Royal Astronomical Society*, **414**, 3699
- Schwarz G., 1978, *Ann. Statist.*, **6**, 461
- Sugar C. A., James G. M., 2003, *Journal of the American Statistical Association*, **98**, 750
- Xu R., Wunsch D. C., 2009, *Clustering*. John Wiley and Sons, Inc, NJ, Hoboken, doi:10.1002/9780470382776

This paper has been typeset from a \LaTeX file prepared by the author.